

LA-UR-15-25933 (Accepted Manuscript)

Dielectric breakdown of additively manufactured polymeric materials

Hayden, Steven

Provided by the author(s) and the Los Alamos National Laboratory (2016-10-19).

To be published in: IEEE Transactions on Dielectrics and Electrical Insulation

DOI to publisher's version: 10.1109/TDEI.2015.005199

Permalink to record: <http://permalink.lanl.gov/object/view?what=info:lanl-repo/lareport/LA-UR-15-25933>

Disclaimer:

Approved for public release. Los Alamos National Laboratory, an affirmative action/equal opportunity employer, is operated by the Los Alamos National Security, LLC for the National Nuclear Security Administration of the U.S. Department of Energy under contract DE-AC52-06NA25396. Los Alamos National Laboratory strongly supports academic freedom and a researcher's right to publish; as an institution, however, the Laboratory does not endorse the viewpoint of a publication or guarantee its technical correctness.

Dielectric Breakdown of Additively Manufactured Polymeric Materials

W. Jacob Monzel, Brad W. Hoff, Sabrina S. Maestas, David M. French

Air Force Research Laboratory
Kirtland AFB
Albuquerque, New Mexico 87117, USA

Steven C. Hayden

Los Alamos National Laboratory
Center for Integrated Nanotechnologies
Los Alamos, New Mexico 87545, USA

ABSTRACT

Dielectric strength testing of selected Polyjet-printed polymer plastics was performed in accordance with ASTM D149. This dielectric strength data is compared to manufacturer-provided dielectric strength data for selected plastics printed using the stereolithography (SLA), fused deposition modeling (FDM), and selective laser sintering (SLS) methods. Tested Polyjet samples demonstrated dielectric strengths as high as 47.5 kV/mm for a 0.5 mm thick sample and 32.12 kV/mm for a 1.0 mm sample. The dielectric strength of the additively manufactured plastics evaluated as part of this study was lower than the majority of non-printed plastics by at least 15% (with the exception of polycarbonate).

Index Terms — **Rapid prototyping, Dielectric breakdown, Plastics, Dielectric materials, Dielectric measurements, Dielectric strength, Additive manufacturing, SLA, Polyjet, Fused Deposition Modeling, FDM, SLS**

1 INTRODUCTION

The field of additive manufacturing (AM) has significantly advanced in the last decade. In additive manufacturing, also called 3D printing or rapid prototyping, layer by layer deposition is used to build up three-dimensional objects. This allows for near net-shape fabrication of parts with complex geometries (to within the resolution of the chosen additive manufacturing process).

The ability to include conductive or metallic traces and other electrical elements within a printed dielectric matrix has enabled complex three dimensional circuit designs to be realized [1, 2]. In the same manner, complex antenna structures can be included within the dielectric walls and structure of a system or vehicle, such as a CubeSat [3], reducing clutter and enhancing overall system compactness.

In order to incorporate 3D-printed circuit elements into devices operating at high voltage, the insulating properties of the printed materials must be known. Here, we examine the dielectric strength of several commonly used printable plastics, deposited by various printing methods. Results are discussed in light of the strengths and weaknesses of these materials in comparison to commonly available non-printed plastics.

1.1 GENERAL DESCRIPTION OF SELECTED ADDITIVE MANUFACTURING METHODS FOR DIELECTRICS

While it is possible to print a wide variety of dielectrics, such as plastics, ceramics [4], or concrete [5], this manuscript focuses on reviewing and evaluating the dielectric strengths of printed plastics from four different processes: Stereolithography (SLA), fused deposition modeling (FDM), Polyjet printing, and selective laser sintering (SLS). Detailed descriptions of these processes are available in the published literature [6, 7, 8] as well as various vendor websites; however, a summary of key aspects of the SLA, FDM, SLS and Polyjet processes is provided forthwith.

The SLA system for manufacturing parts involves a tank of curable liquid photopolymer resin and an elevator platform to control the cured component height and define the layer thickness. An ultraviolet laser is used to cure the desired regions of the liquid, thereby fusing it to the previously solidified layer. The elevator platform is then lowered and the next layer can be built, thereby building the desired part from the bottom up. SLA can provide layer thickness little as 0.05 mm, enabling the production of high-resolution features on printed parts. When the part has been completed, it is given a chemical bath to wash off excess material. Once the bath is

complete, the part is then put into an oven to be cured. SLA machines require concurrent printing of support structures to facilitate attachment of the part to the elevator platform and shape retention in the force of gravity. After printing, the support structures are manually removed from the finished product.

As in SLA, FDM also generates structures via bottom-up, layer-by-layer deposition. FDM differs from SLA in that each layer of the part is built using a nozzle that dispenses material in liquid form. A digital template file is used to direct the path of the nozzle and ultimately define the shape of the printed part. Like SLA, FDM also necessitates the use of support structures. However, whereas in SLA the support is built into the part and later mechanically removed, in FDM, a different material is dispensed to build the support structures. Upon completion of the part, a chemical bath is used to dissolve the temporary support material laid during the printing process. An FDM machine can generate layers as thin as 0.18 mm, and, while the precision is decreased relative to SLA, FDM printing tends to be less expensive.

Polyjet printers also utilize jets / nozzles to direct material layer deposition. In Polyjet printing, parts are built one layer at a time from the bottom up in a manner similar to that of an Inkjet printer, and the process provides a minimum available layer thickness of 0.015 mm. The Polyjet process utilizes an elevator platform and support material like other systems; this support material is removed immediately following part completion using a jet of water. Unfortunately, the use of a water jet to remove support structures potentially limits the use of Polyjet printing for the fabrication of fragile parts, as the water jet can have deleterious effects on part structure. However, an advantage of Polyjet printing lies in its ability to layer two different plastics in a single part.

The SLS process differs from other 3D printing systems in its use of powders – instead of fluids – for material deposition. These powders can be plastic, metal, glass or ceramic, making SLS a very versatile option for 3D printing. SLS uses a high power laser to fuse the particles of the chosen material together and incorporates the same type of elevator platform used in SLA to build the part from the bottom up. Each time the platform is lowered, a new layer of powder is laid over the previous layer, and the laser continues to fuse the particles until the finished part is created. As part of the SLS process, the part being manufactured is supported by the surrounding unfused powder; thus printed support structures are not necessary. The finished part is removed from the powder block with brushes in a clean environment, and the unused powder can be recycled for use in future parts. Layer thicknesses for current SLS printers can be as small as 0.1 mm.

2 DIELECTRIC STRENGTH TESTING OF POLYJET SAMPLES

Because dielectric strength data was not available for currently available Stratasys Polyjet resins [9], sets of five 1.0-

mm-thick tiles and five 0.5-mm-thick tiles (5.08 cm x 5.08 cm, W x H) were printed with an Objet 500 Connex2 at 16 micron resolution using the ABS Green, DurusWhite, TangoBlackPlus, Transparent RGD720, VeroBlue, and VeroClear resins. Prior to testing, each of the samples was cleaned via gentle abrasion while immersed in Liquinox (aq., 1% solution)). Following six rinses with deionized water, samples were placed between sheets of lint-free tissue and allowed to air dry at ambient temperature. Dry samples were stored between clean sheets of lint-free tissue in a desiccated environment and were thus transported to the testing laboratory.

Just prior to testing, the samples were pre-conditioned for 40 hours at 23 °C and 50% relative humidity. All samples were tested per ASTM D149-09 (2013), Paragraph 12.2.1, Method A (short time test) [10] using 2.54 cm diameter stainless steel electrodes (ASTM “Type 2” electrodes) in a transformer oil bath. Ambient room conditions during testing were 24 °C and 36% relative humidity.

Results of the dielectric strength testing are plotted in Figure 1. The error bars represent one standard deviation. The observed difference in measured dielectric strength between the 0.5 mm and 1.0 mm samples is expected, as the measured dielectric strength for relatively homogeneous, solid material is expected to vary as the reciprocal of the square root of the specimen thickness (per ASTM D149-09 (2013) Appendix X1 (Paragraph X1.4.2)).

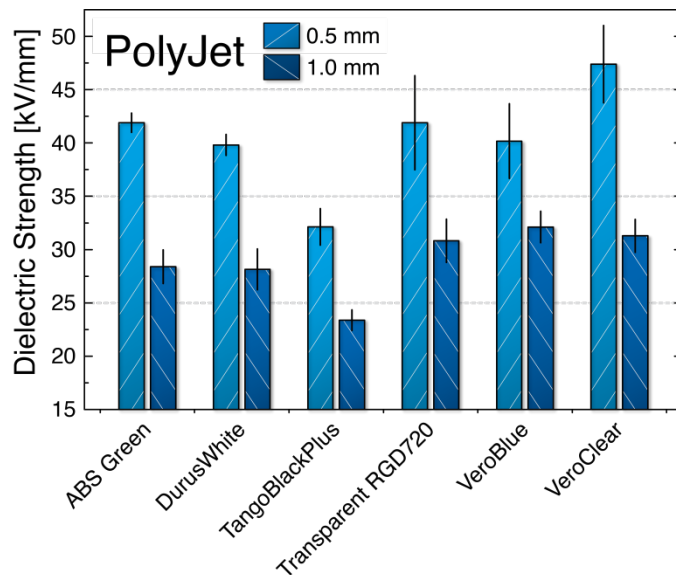


Figure 1. ASTM D149 dielectric strength testing data for 0.5 mm (light blue) and 1.0 mm (dark blue) sample thicknesses of additively manufactured Polyjet resins.

As shown in Figure 2, when sample thickness is compensated for by multiplying the measured dielectric strength value by the square root of the sample thickness, the dielectric strength values from the 0.5 mm thick and 1.0 mm thick cases are equivalent within error. The average of the thickness-compensated data for each material is also plotted. While this

“thickness compensated” dielectric strength value (having units of $\text{kV/mm}^{0.5}$) is not the typical definition of dielectric strength (having units of kV/mm), it does allow for comparison between data sets in which different sample thicknesses were utilized, within the assumptions discussed in Ref. [10].

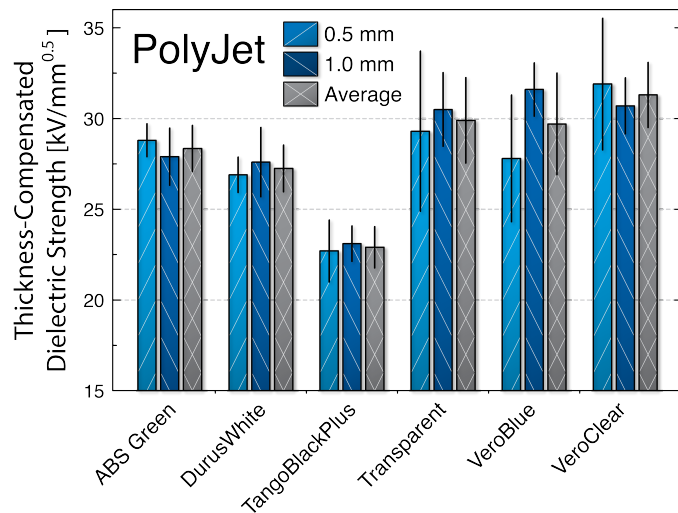


Figure 2. Thickness compensated dielectric strength values of assayed PolyJet resins of 0.5 mm (light blue) and 1.0 mm (dark blue) thickness and the average of these (grey).

3 DIELECTRIC STRENGTH COMPARISONS OF PRINTED PLASTICS

In order to compare the dielectric strength of the Polyjet resins to other printed plastics, manufacturer data was gathered for printed plastics from the SLS, FDM, and SLA processes [11-40]. All manufacturer data presented here were acquired in accordance with the ASTM D149 standard. Manufacturer sample thickness used in dielectric strength testing was not provided in the manufacturer data but was obtained via correspondence with the manufacturers [41, 42]. Further correspondence [43, 44] yielded previously unpublished information on electrode configuration, test medium, and sample pre-conditioning for FDM and SLA testing, but could not be obtained for the SLS samples. FDM and SLA samples were both pre-conditioned for 40 hours at 23 °C and 50% relative humidity and were tested in oil. The FDM testing was performed using ASTM “Type 1” electrodes (5.08 cm in diameter) and the SLA samples were tested using ASTM “Type 3” electrodes (0.64 cm in diameter). Tabulated data for selected materials are provided in the Appendix.

The authors note that dielectric strength testing of a limited number of SLA resins has been performed by Peterkin, et al. [45]; however, because Peterkin, et al. did not utilize the standardized ASTM D149 testing procedure, data from this study are not discussed in the present manuscript.

Different material manufacturers tend to choose different sample thicknesses on which to perform the ASTM D149 testing, therefore, the manufacturer data were compensated for

thickness by multiplying the dielectric strength by the square root of the sample thickness, as described previously. Data from printed SLS and FDM resins are presented in Figure 3. The FDM data is split into “upright” (ZX direction) printing orientation and “on-edge” (XZ direction) orientation, as described by the manufacturer in Ref. [46, 47]. Data from printed SLA resins with various ultra violet (UV) light and thermal post treatments are plotted in Figure 4.

As a group, the worst performing printed plastics were found to be those fabricated using FDM in the XZ printing direction. It is possible that the disparity of dielectric strengths of the FDM materials in different printing directions is related to the large number and alignment of voids that are left between the extruded cylinders of thermoplastic that comprise the printed shape. The heterogeneity of sample properties caused by the orientation of these extruded cylinders may be related to the range of values for a given resin published in the FDM resin manufacturer data [31-40, 45-50].

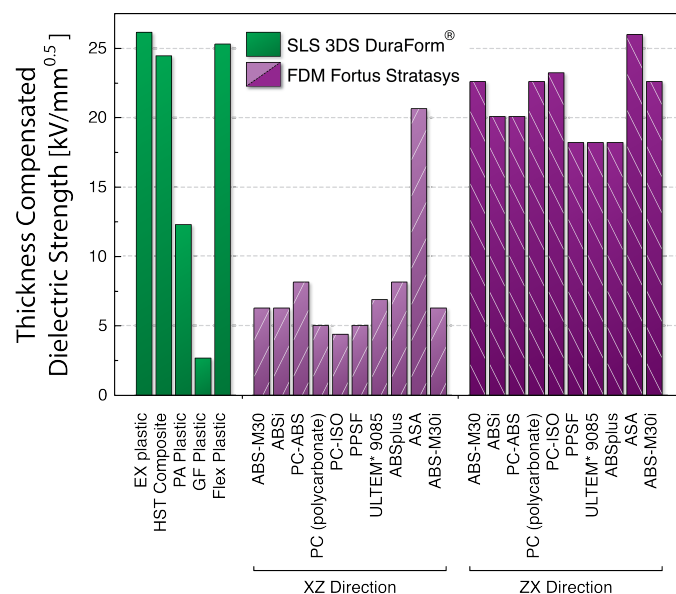


Figure 3. Thickness compensated dielectric strength data for printed SLS resins (green) and printed FDM resins (purple) printed in the XZ and ZX directions, as indicated.

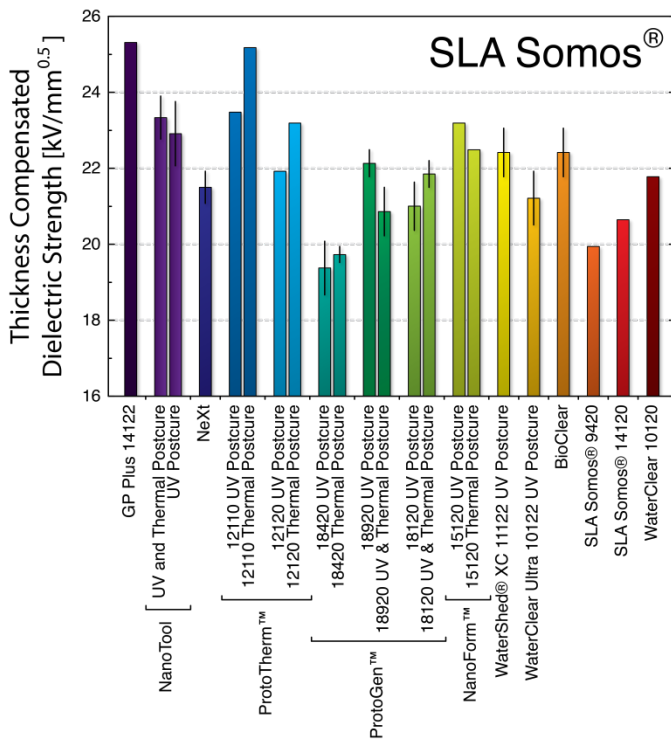


Figure 4. Thickness compensated dielectric strength values for printed SLA resins.

The SLS plastics exhibited a mix of good and extremely poor-performing sample data. It is unknown at this time the reason for the extremely poor performance of the DuraForm GF plastic.

With the exception of the TangoBlackPlus rubber-like resin, the printed Polyjet samples tested as part of this study exhibited the highest dielectric strengths of any of the other three material groups evaluated. The SLA resins, while exhibiting lower dielectric strengths than the Polyjet plastics, were found to be very consistent across the group. The thermal and UV post-treatments commonly applied to SLA printed components, appeared to have little overall effect on the dielectric strength.

To facilitate comparison of printed plastics with commonly available non-printed plastics, Figure 5 has been provided. Material data was sourced from [51]. With the exception of polycarbonate, the published dielectric strength of these standard plastics exceed that of the best performing additive plastic evaluated (Polyjet VeroClear) by ~15% or more. This observed discrepancy in dielectric strength is likely due to a combination of a large number of factors, including innate material differences (*i.e.*, comparisons between photopolymers and thermoplastics), void inclusion during printing, and possible changes in resin formulation used to enhance printability. A more detailed study of these factors would likely be necessary to determine an effective path forward in enhancing the dielectric strength of printed materials.

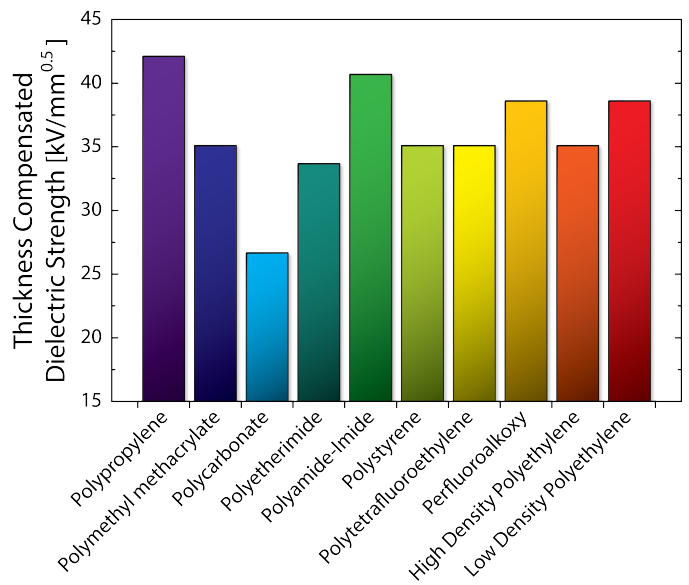


Figure 5. Thickness compensated dielectric strength values for standard plastics.

4 SUMMARY AND DISCUSSION

Samples printed from six different Polyjet resins were tested according to the ASTM D149-09 (2013) standard. These data were then compared to published manufacturer data for plastics printed using the SLS, FDM, and SLA processes. It is important to note that due to the differences in ASTM test electrodes used by different manufacturers (in the cases where this information could be obtained by the authors), comparisons between sets of data from different manufacturers must be considered qualitative. The ASTM D149 standard indicates that breakdown is expected to decrease with increasing electrode area (with the area effect being more pronounced with decreasing sample thickness); however, no specific method of compensation to allow direct comparisons of data from different electrode configurations is provided [10].

Within the limited confidence allowed by the aforementioned caveats for comparing data taken with different electrode types, the Polyjet plastics were found to have the highest dielectric strengths of any of the other printed sample types, excepting the Polyjet printed TangoBlackPlus resin. The best performing printed plastic was found to be the Polyjet VeroClear with a thickness compensated dielectric strength value of 31.3 kV/mm^{0.5}.

The dielectric strength of the additively manufactured plastics evaluated as part of this study was lower than the majority of non-printed plastics by at least 15% (with the exception of polycarbonate). In general, the data suggest that when insulating plastics are required in a given high voltage application requiring high dielectric strength insulators and standard subtractive machining processes are viable, a printed insulator would likely be less desirable due to reduced dielectric strength. In cases where insulator complexity begins to exceed the capabilities of subtractive machining processes,

a printed insulator would be a more competitive choice.

ACKNOWLEDGMENT

W. J. Monzel's participation in this work was accomplished under the Air Force Research Laboratory Directed Energy Summer Scholars Program. Funding for this work was provided by the Air Force Research Laboratory. S. C. Hayden's participation in this work was performed, in part, at the Center for Integrated Nanotechnologies, an Office of Science User Facility operated for the U.S. Department of Energy (DOE) Office of Science. Los Alamos National Laboratory, an affirmative action equal opportunity employer, is operated by Los Alamos National Security, LLC, for the National Nuclear Security Administration of the U.S. Department of Energy under contract DE-AC52-06NA25396. Polyjet sample testing was performed at Element Materials Technology (www.element.com).

REFERENCES

- [1] D. Espalin, D. W. Muse, E. MacDonald, and R. B. Wicker, "3D Printing multifunctionality: structures with electronics," *Int. J. Adv. Manuf. Technol.* (2014) 72:963-978.
- [2] E. MacDonald, R. Salas, D. Espalin, M. Perez, E. Aguilera, D. Muse, and R. B. Wicker, "3D Printing for the Rapid Prototyping of Structural Electronics," *IEEE Access*, vol.2, pp.234-242, Dec. 2014.
- [3] A. Kwas, E. MacDonald, C. J. Kief, R. Wicker, C. Soto, L. Banuelos, J. Aarestad, B. Zufelt, J. D. Stegeman, and C. Tolbert, "Printing Multi-Functionality: Additive Manufacturing for CubeSats," 2014 AIAA SPACE Conference and Exposition, August 2014.
- [4] Y. Hagedorn, J. Wilkes, W. Meiners, K. Wissenbach, and R. Poprawe, "Net Shaped High Performance Oxide Ceramic Parts by Selective Laser Melting," *Proceedings of the LANE 2010*, Vol. 5, Part B, 2010, 587-594.
- [5] S. Lim, R. A. Buswell, T. T. Le, S. A. Austin, A. G. F. Gibb, and T. Thorpe, "Developments in construction-scale additive manufacturing processes," *Automation in Construction* 21 (2012), 262-268.
- [6] C. B. Williams, F. Mistree, and D. W. Rosen, "A Functional classification framework for the conceptual design of additive manufacturing technologies," *Journal of Mechanical Design*, vol. 133, no. 12, 121002 (11 pp.), Dec. 2011
- [7] N. Tukur, S. Gowda, S. M. Ahmed, and S. Badami, "Rapid Prototype Technique in Medical Field," *Research J. Pharm. And Tech.* 1(4): Oct-Dec. 2008.
- [8] K. V. Wong and A. Hernandez, "A Review of Additive Manufacturing," *ISRN Mechanical Engineering*, vol. 2012, 208760.
- [9] Stratays, Ltd. "Polyjet Materials Data Sheet" 2014.
- [10] Standard Test Method for Dielectric Breakdown Voltage and Dielectric Strength of Solid Electrical Insulating Materials at Commercial Power Frequencies, ASTM D149 - 09, 2013
- [11] 3D Systems, Inc, "DuraForm® EX plastic," datasheet, 2008 [Revised June 2011].
- [12] 3D Systems, Inc, "DuraForm® HST Composite," datasheet, 2008 [Revised June 2011].
- [13] 3D Systems, Inc, "DuraForm® PA Plastic," datasheet, 2010 [Revised June 2011].
- [14] 3D Systems, Inc, "DuraForm® GF Plastic," datasheet, Mar. 2012.
- [15] 3D Systems, Inc, "DuraForm® Flex Plastic," datasheet, Feb. 2012.
- [16] Royal DSM, "Somos® GP Plus 14122," datasheet, 2012 [Revised Nov. 2013].
- [17] Royal DSM, "Somos® NanoTool," datasheet, 2012 [Revised Nov. 2013].
- [18] Royal DSM, "Somos® NeXt," datasheet, 2012 [Revised Nov. 2013].
- [19] Royal DSM, "Somos® ProtoTherm™ 12110," datasheet, 2012 [Revised Nov. 2013].
- [20] Royal DSM, "Somos® ProtoTherm™ 12120," datasheet, 2012 [Revised Nov. 2013].
- [21] Royal DSM, "Somos® ProtoGen™ 18420," datasheet, Apr. 2012.
- [22] Royal DSM, "Somos® ProtoGen™ 18920," datasheet, Apr. 2012.
- [23] Royal DSM, "Somos® ProtoGen™ 18120," datasheet, Apr. 2012.
- [24] Royal DSM, "Somos® NanoForm™ 15120," datasheet, Nov. 2005 [Revised Mar. 2009].
- [25] Royal DSM, "Somos® WaterShed® XC 11122," datasheet, 2012 [Revised Nov. 2013].
- [26] Royal DSM, "Somos® WaterClear Ultra 10122," datasheet, 2012 [Revised Nov. 2013].
- [27] Royal DSM, "Somos® BioClear," datasheet, 2012 [Revised Nov. 2013].
- [28] Royal DSM, "Somos® 9420," datasheet, 2012 [Revised Nov. 2013].
- [29] Royal DSM, "Somos® 14120," datasheet, 2012 [Revised Nov. 2013].
- [30] Royal DSM, "WaterClear 10120," datasheet, 2012 [Revised Nov. 2013].
- [31] Stratays Inc., "FortusABSM30MaterialSpecSheet-US-09-14," datasheet, Sept. 2014.
- [32] Stratays Inc., "FortusABSiMaterialSpecSheet-US-09-14," datasheet Sept. 2014.
- [33] Stratays Inc., "FortusPCABSMaterialSpecSheet-US-09-14," datasheet, Sept. 2014.
- [34] Stratays Inc., "FortusPCMaterialSpecSheet-US-09-14," datasheet, Sept. 2014.
- [35] Stratays Inc., "FortusPCISOMaterialSpecSheet-US-09-14," datasheet, Sept. 2014.
- [36] Stratays Inc., "FortusPPSFMaterialSpecSheet-US-09-14," datasheet, Sept. 2014.
- [37] Stratays Inc., "FortusUltem9085MaterialSpecSheet-US-09-14," datasheet, Sept. 2014.
- [38] Stratays Inc., "SSYS-ABSplusP430-MaterialSpecSheet-EN-11-14," datasheet, Nov. 2014
- [39] Stratays Inc., "SSYS-ASAMaterialSpecSheet-EN-09-14," datasheet, Sept. 2014.
- [40] Stratays Inc., "FortusABSM30iMaterialSpecSheet-US-09-14," datasheet, Sept. 2014.
- [41] G. Camacho, Royal DSM. Telephone Conversation (3 Nov. 2014)
- [42] K. Hayes, "Re: question about dielectric strength data," Personal E-mail (4 Nov., 2014).
- [43] B. Baggerly, "Re: Question," Personal E-mail (18 May, 2015).
- [44] G. Camacho, "Re: ASTM D 149," Personal E-mail (15 May, 2015).
- [45] F. E. Peterkin, J. L. Stevens, J. F. Sharrow, and R. K. Pitman, "High voltage breakdown strength of rapid prototype materials," *Pulsed Power Conference, 2003. Digest of Technical Papers. PPC-2003. 14th IEEE International*, vol.2, pp.1025-1028, 15-18 June 2003
- [46] Stratays, Inc., "SSYS-MS-PC-PropertiesReport-01/13," white paper, Jan. 2013.
- [47] Stratays, Inc., "SSYS-MS-ABS-M30-PropertiesReport-01/13," white paper, Jan. 2013.
- [48] I. Gajdos and J. Slota, "Influence of printing conditions on structure in FDM prototypes," *Tehnicki vjesnik*, vol. 20, no. 2, 231 – 236, 2013.
- [49] Zhang, Yu, "Mechanical property of fused deposition parts" Theses and Dissertations, Lehigh Preserve, Lehigh University (2002).
- [50] Swetly T, Stampfl J, Kempf G, Hucke R (2014). Capabilities of additive manufacturing technologies (AMT) in the validation of the automotive cockpit. *RTEjournal - Forum für Rapid Technologie*, Vol. 2014.
- [51] W. T. Shugg, *Handbook of Electrical and Electronic Insulating Materials, 2nd Ed.* IEEE Press: New Jersey, 1995



W. Jacob Monzel was born in North Carolina, USA, in 1989. He received a B.S. and M.S. degrees in Materials Science and Engineering from Virginia Polytechnic Institute and State University (Virginia Tech), USA in 2011 and 2014 respectively. He is currently pursuing a Ph.D. degree, also at Virginia Tech, under the Science, Mathematics and Research for Transformation (SMART) Scholarship for Service Program. He has interned under The Air Force Research Laboratory Directed Energy Scholars

Program and for Corning Inc. He has also worked as a Materials Engineer for Theta Tech Solutions LLC.



Brad W. Hoff (S'04–M'10) received the B.S. degree in physics from the U.S. Naval Academy, Annapolis, MD, USA, in 1999 and the M.S.E. degree in nuclear engineering, the M.S.E. degree in electrical engineering, and the Ph.D. degree in nuclear engineering from the University of Michigan, Ann Arbor, MI, USA, in 2006, 2007, and 2009, respectively. He is currently a Research Physicist with the Directed Energy Directorate, Air Force Research Laboratory, Kirtland Air Force Base, Albuquerque, NM, USA. His research interests include high-power microwave sources and applications of additive manufacturing to directed energy technology.



David M. French (S'07–M'11) received a B.S. in physics in 2006 from Colorado State University, Fort Collins, CO. He received M.S (2008) and Ph.D. (2011) degrees in nuclear science from the University of Michigan, Ann Arbor. He joined the Air Force Research Laboratory Directed Energy Directorate in 2011 where his research focuses on high power electromagnetics and related technologies.

Sabrina Maestas was born in New Mexico, USA, in 1984. She received a B.S. degree in Mechanical Engineering from the University of New Mexico, Albuquerque, NM, USA, in 2008. She is currently a Mechanical Engineer with the Directed Energy Directorate, Air Force Research Laboratory, Kirtland Air Force Base, Albuquerque, NM, USA.



Steven C. Hayden was born in Georgia, USA, in 1982. He attained bachelor's degrees in Chemistry and French Language from Mercer University in 2004, after which he joined the Children's Exposure to Environmental Pesticides (CEEP) research team at the Centers for Disease Control and Prevention (CDC) in Atlanta. In 2007, Steven began his doctoral research at Georgia Institute of Technology, where he integrated plasmonic nanomaterials into biotic/biomimetic systems for applications in solar energy conversion and cancer therapeutics. After completion of his PhD in Chemistry & Biochemistry in 2012 (GA Tech), Steven briefly sojourned to the University of Heidelberg in Germany, where he helped develop the nanosynthetic capabilities of the University. In 2013, Steven joined the Center for Integrated Nanotechnologies at Los Alamos National Lab, where he is currently studying the use of self-assembling, mesostructured matrices to arrange both synthetic and natural nanospecies in an effort to generate responsive composites with emergent, tunable optical and electronic properties.

Appendix

Table 1. Dielectric strengths and thickness-compensated dielectric strengths of selected PolyJet plastics (ASTM "Type 2" electrodes).

PolyJet Plastics	Dielectric Strength [kV/mm] (per ASTM D149)	Error (+/-) [kV/mm] (if available)	Specified Sample Thickness [mm]	Thickness Compensated Dielectric Strength [kV/mm ²] (per ASTM D149)	Thickness Compensated Error (+/-) [kV/mm ²] (if available)	References
PolyJet ABS Green (0.5 mm)	41.90	0.90	0.50	28.80	0.90	[9]
PolyJet ABS Green (1.0mm)	28.39	1.57	1.00	27.90	1.57	[9]
PolyJet ABS Green (Average)				28.35	1.28	[9]
PolyJet DurusWhite (0.5mm)	39.81	0.98	0.50	26.90	0.98	[9]
PolyJet DurusWhite (1.0mm)	28.14	1.91	1.00	27.60	1.91	[9]
PolyJet DurusWhite (Average)				27.25	1.29	[9]
PolyJet TangoBlackPlus (0.5 mm)	32.13	1.70	0.50	22.70	1.70	[9]
PolyJet TangoBlackPlus (1.0 mm)	23.37	0.97	1.00	23.10	0.97	[9]
PolyJet TangoBlackPlus (Average)				22.90	1.14	[9]
PolyJet Transparent RGD720 (0.5 mm)	41.90	4.42	0.50	29.30	4.42	[9]
PolyJet Transparent RGD720 (1.0 mm)	30.82	2.03	1.00	30.50	2.03	[9]
PolyJet Transparent (Average)				29.90	2.35	[9]
PolyJet VeroBlue (0.5 mm)	40.18	3.49	0.50	27.80	3.49	[9]
PolyJet VeroBlue (1.0 mm)	32.12	1.47	1.00	31.60	1.47	[9]
PolyJet VeroBlue (Average)				29.70	2.81	[9]
PolyJet VeroClear (0.5 mm)	47.40	3.63	0.50	31.90	3.63	[9]
PolyJet VeroClear (1.0 mm)	31.29	1.54	1.00	30.70	1.54	[9]
PolyJet VeroClear (Average)				31.30	1.79	[9]

Table 2. Dielectric strengths and thickness-compensated dielectric strengths of selected SLS plastics (unknown electrode configuration).

	Dielectric Strength [kV/mm] (per ASTM D149)	Error (+/-) [kV/mm] (if available)	Sample Thickness [mm]	Thickness Compensated Dielectric Strength [kV/mm ^{1/3}] (per ASTM D149)	Thickness Compensated Error (+/-) [kV/mm ^{1/3}] (if available)	References
SLS Plastics						
SLS 3DS DuraForm® EX plastic	18.5		2.0	26.2		[11], [42]
SLS 3DS DuraForm® HST Composite	18.5		3.5	26.2		[12], [42]
SLS 3DS DuraForm® PA Plastic	17.3		2.0	24.5		[13], [42]
SLS 3DS DuraForm® GF Plastic	8.7		2.0	12.3		[14], [42]
SLS 3DS DuraForm® Flex Plastic	1.9		2.0	2.7		[15], [42]

Table 3. Dielectric strengths and thickness-compensated dielectric strengths of selected SLA plastics (ASTM “Type 3” electrodes).

	Dielectric Strength [kV/mm] (per ASTM D149)	Error (+/-) [kV/mm] (if available)	Sample Thickness [mm]	Thickness Compensated Dielectric Strength [kV/mm ^{1/3}] (per ASTM D149)	Thickness Compensated Error (+/-) [kV/mm ^{1/3}] (if available)	References
SLA Plastics						
SLA Somos® GP Plus 14122	17.9		1.587	25.3		[16], [41]
SLA Somos® NanoTool UV and Thermal Postcure	16.1	0.4	1.587	23.3	0.6	[17], [41]
SLA Somos® NanoTool UV Postcure	15.6	0.6	1.587	22.9	0.8	[17], [41]
SLA Somos® NeXt	14.9	0.3	1.587	21.5	0.4	[18], [41]
SLA Somos® ProtoTherm 12110 UV Postcure	16.6		1.587	23.5		[19], [41]
SLA Somos® ProtoTherm 12110 Thermal Postcure	17.8		1.587	25.2		[19], [41]
SLA Somos ProtoTherm™ 12120 UV Postcure	15.5		1.587	21.9		[20], [41]
SLA Somos ProtoTherm™ 12120 Thermal Postcure	16.4		1.587	23.2		[20], [41]
SLA Somos ProtoGen™ 18420 UV Postcure	13.2	0.5	1.587	19.4	0.7	[21], [41]
SLA Somos ProtoGen™ 18420 Thermal Postcure	13.8	0.2	1.587	19.7	0.2	[21], [41]
SLA Somos ProtoGen™ 18920 UV Postcure	15.4	0.3	1.587	22.1	0.4	[22], [41]
SLA Somos ProtoGen™ 18920 UV & Thermal Postcure	14.3	0.4	1.587	20.9	0.6	[22], [41]
SLA Somos® ProtoGen 18120 UV Postcure	14.4	0.4	1.587	21.0	0.6	[23], [41]
SLA Somos® ProtoGen 18120 UV & Thermal Postcure	15.2	0.3	1.587	21.8	0.4	[23], [41]
SLA Somos NanoForm™ 15120 UV Postcure	16.4		1.587	23.2		[24], [41]
SLA Somos NanoForm™ 15120 Thermal Postcure	15.9		1.587	22.5		[24], [41]
SLA Somos WaterShed® XC 11122 UV Postcure	15.4	0.4	1.587	22.4	0.6	[25], [41]
SLA Somos® WaterClear Ultra 10122 UV Postcure	14.5	0.5	1.587	21.2	0.7	[26], [41]
SLA Somos® BioClear	15.4	0.4	1.587	22.4	0.6	[27], [41]
SLA Somos® 9420	14.1		1.587	19.9		[28], [41]
SLA Somos® 14120	14.6		1.587	20.6		[29], [41]
SLA Somos® WaterClear 10120	15.4		1.587	21.8		[30], [41]

Table 4. Dielectric strengths and thickness-compensated dielectric strengths of selected FDM plastics printed in the XZ direction (ASTM “Type 1” electrodes).

	Dielectric Strength [kV/mm] (per ASTM D149)	Error (+/-) [kV/mm] (if available)	Sample Thickness [mm]	Thickness Compensated Dielectric Strength [kV/mm ^{1/3}] (per ASTM D149)	Thickness Compensated Error (+/-) [kV/mm ^{1/3}] (if available)	References
FDM Plastics (XZ Direction)						
FDM Fortus Stratasys ABS-M30	3.9		2.5	6.3		[31]
FDM Fortus Stratasys ABSi	3.9		2.5	6.3		[32]
FDM Fortus Stratasys PC-ABS	5.1		2.5	8.2		[33]
FDM Fortus Stratasys PC (polycarbonate)	3.2		2.5	5.0		[34]
FDM Fortus Stratasys PC-ISO	2.8		2.5	4.4		[35]
FDM Fortus Stratasys PPSF	3.2		2.5	5.0		[36]
FDM Fortus Stratasys ULTEM® 9085	4.3		2.5	6.9		[37]
FDM Fortus Stratasys ABSplus	5.1		2.5	8.2		[38]
FDM Fortus Stratasys ASA	13.0		2.5	20.7		[39]
FDM Fortus Stratasys ABS-M30i	3.9		2.5	6.3		[40]

Table 5. Dielectric strengths and thickness-compensated dielectric strengths of selected FDM plastics printed in the ZX direction (ASTM “Type 1” electrodes).

	Dielectric Strength [kV/mm] (per ASTM D149)	Error (+/-) [kV/mm] (if available)	Sample Thickness [mm]	Thickness Compensated Dielectric Strength [kV/mm ^{1/3}] (per ASTM D149)	Thickness Compensated Error (+/-) [kV/mm ^{1/3}] (if available)	References
FDM Plastics (ZX Direction)						
FDM Fortus Stratasys ABS-M30	14.2		2.5	22.6		[31]
FDM Fortus Stratasys ABSi	12.6		2.5	20.1		[32]
FDM Fortus Stratasys PC-ABS	12.6		2.5	20.1		[33]
FDM Fortus Stratasys PC (polycarbonate)	14.2		2.5	22.6		[34]
FDM Fortus Stratasys PC-ISO	14.6		2.5	23.2		[35]
FDM Fortus Stratasys PPSF	11.4		2.5	18.2		[36]
FDM Fortus Stratasys ULTEM® 9085	11.4		2.5	18.2		[37]
FDM Fortus Stratasys ABSplus	11.4		2.5	18.2		[38]
FDM Fortus Stratasys ASA	16.3		2.5	26.0		[39]
FDM Fortus Stratasys ABS-M30i	14.2		2.5	22.6		[40]

Table 6. Dielectric strengths and thickness-compensated dielectric strengths of selected conventional plastics (unknown electrode configuration).

Conventional Plastics

	Dielectric Strength [kV/mm] (per ASTM D149)	Error (+/-) [kV/mm] (if available)	Sample Thickness (mm)	Thickness Compensated Dielectric Strength [kV/mm ^{0.5}] (per ASTM D149)	Thickness Compensated Error (+/-) [kV/mm ^{0.5}] (if available)	References
Polypropylene	23.6		3.175	42.1		[51]
Polymethyl methacrylate (Acrylic, PMMA)	19.7		3.175	35.1		[51]
Polycarbonate	15.0		3.175	26.7		[51]
Polyetherimide (PEI, Ultem)	18.9		3.175	33.7		[51]
Polyamide-Imide	22.8		3.175	40.7		[51]
Polystyrene	19.7		3.175	35.1		[51]
Polytetrafluoroethylene (PTFE, Teflon)	19.7		3.175	35.1		[51]
Perfluoroalkoxy (PFA, Teflon)	21.7		3.175	38.6		[51]
High Density Polyethylene (HDPE)	19.7		3.175	35.1		[51]
Low Density Polyethylene (LDPE)	21.7		3.175	38.6		[51]